N_3 = salt mole fraction in the ethanol–water–potassium acetate liquid phase = (mol of potassium acetate)/(mol of potassium acetate + mol of ethanol + mol of water)
N_3' = salt mole fraction in the ethanol–water–salt mixtures liquid phase = (mol of potassium acetate + mol of sodium acetate)/(mol of potassium acetate + mol of sodium acetate + mol of ethanol + mol of water)
P = system pressure (mmHg)
P°_i = vapor pressure of pure component i (mmHg)
P^*_i = corrected vapor pressure of component i (mmHg)
T = temperature liquid phase (°C)
x_i = mole fraction of component i in the liquid phase, calculated on a salt free basis = (mol of ethanol or water)/(mol of ethanol + mol of water)
y_i = mole fraction of component i in the vapor phase = (mol of ethanol or water)/(mol of ethanol + mol of water)
α_s = relative volatility of ethanol in the presence of the salt
γ_i = activity coefficient in the liquid phase of component i
ϵ_2 = vapor pressure correction factor for the calculation of the activity coefficient

Literature Cited

(1) Gorhan, A. U.S. Pat. 1879847, 1932; *Chem. Abstr.* **1933**, *27*, 369.
(2) Furter, W. F. ACS 160th National Meeting, Chicago, IL, Sept 1970.
(3) Meranda, D.; Furter, W. F. *Can. J. Chem. Eng.* **1966**, *44* (5), 298.
(4) Cook, R. A.; Furter, W. F. *Can. J. Chem. Eng.* **1968**, *46*, 119.
(5) Costa Novella, E.; Moragues Tarrasó, J. *An. R. Soc. Esp. Fis. Quim.* **1952**, *48B*, 441.
(6) Meranda, D.; Furter, W. F. *AIChE J.* **1971**, *17*, 38.
(7) Michalowski, S.; Mondaja, D. *Cent. Azucar* **1977**, *4* (3), 25.
(8) Johnson, A. I.; Furter, W. F. *Can. J. Chem. Eng.* **1965**, *43*, 356.
(9) Sabarathinam, P. L.; Andiappan, A. N.; Lakshmanan, S. M. *Chem. Ind. Dev.* **1975**, *9*, 27.
(10) Schmitt, D. Ph.D. Thesis, University of Karlsruhe, Germany, 1979.
(11) Walas, S. M. *Phase Equilibria in Chemical Engineering*; Butterworth: London, 1985.
(12) Gmehling, J.; Onken, U.; Arlt, W. *Vapor-Liquid Equilibrium Data Collection*; DECHEMA: Frankfurt, 1981; Vol. I/1.
(13) Jaques, D.; Furter, W. F. *AIChE J.* **1972**, *18*, 343.
(14) Natarajan, T. S.; Srinivasan, D. *J. Chem. Eng. Data* **1980**, *25*, 215.

Received for review May 15, 1990. Revised January 14, 1991. Accepted February 6, 1991.

Densities and Viscosities of NH_4Br–NH_3 and NH_4I–NH_3 Systems

Hideki Yamamoto* and Junji Tokunaga*

Department of Chemical Engineering, Faculty of Engineering, Kansai University, Yamate-cho, Suita, Osaka, 564 Japan

Densities of the NH_4Br–NH_3 and NH_4I–NH_3 systems in liquid phase have been measured over a wide range of temperatures and concentrations. Densities of saturated solutions of the NH_4Br–NH_3 and NH_4I–NH_3 systems have also been measured over the temperature range from 0 to 76.5 °C and from 0 to 69.5 °C, respectively. The accuracy of this measurement was ±0.1%. Observed densities were expressed as a function of temperature and concentration by means of polynomial equations. These equations could calculate values to an accuracy within ±0.5% of the observed data. For the sake of the viscometry of these systems, a falling-body viscometer with use of a He–Ne laser was assembled. The viscosities of NH_4Br–NH_3 and NH_4I–NH_3 systems were measured in the ranges of mass percent of ammonium halide from 10.0% to 59.8% and from 9.81% to 70.1% under the wide temperature range respectively. The accuracy of these viscometry was within ±1.2% deviation against standard liquid to calibrate this viscometer.

Introduction

Very little information for the physical properties of ammoniated salts in the liquid phase is available for the concentrated solution. Most of the investigations of ammonium salts in the literature involve mainly aqueous solutions. Although dilute aqueous solutions have greatly contributed to the development of physical chemistry, the behavior of concentrated nonaqueous electrolytic solutions has not yet been completely investigated. Progress in theoretical descriptions of these ammoniated salts requires the availability of experimentally determined data.

In recent years, some ammoniated salts were used as working system for chemical heat pumps and energy storage (*1*, *2*). However, most of the studies in the literature involving ammoniated salts have been carried out at or near normal boiling point to avoid experimentation at high pressures. Some physical and thermodynamic properties of NH_4Br–NH_3 and NH_4I–NH_3 (i.e. vapor pressures, solubilities, specific heats, and heats of mixing) were already measured in this laboratory (*3*, *4*).

In this paper, the densities in the wide temperature and concentration ranges were measured by using the special equipment that was made to facilitate measurements at high pressure. Observed densities were expressed as the function of temperature and concentration, using the method of least-squares. Furthermore, the viscosities of these systems were measured by using the falling-body viscometer, which was specially assembled for the measurement of the solution under high pressure. This paper is concerned with the densities and viscosities of the NH_4Br–NH_3 and NH_4I–NH_3 systems.

Materials. Ammonium iodide (NH_4I) and ammonium bromide (NH_4Br) from Wako Pure Chemical Industries, Ltd., were of guaranteed reagent grade and were specified as the pure grade, having minimum purities of 99.5%, and used without further purification. The powdered crystal was thoroughly dried at 100 °C and stored over silica gel in a desiccator. Ammonia gas of 99.99% purity was provided by Seitetu Kagaku Co., Ltd.

The standard liquid for calibration viscometers was used in order to examine the accuracy of the falling-body viscometer from Showa Shell Sekiyu Co., Ltd. The range of viscosities for the standard liquid was 0.1–5.0 Pa s.

Apparatus and Procedures

Density Measurement. A schematic diagram of the experimental apparatus for density measurements is shown in Figure 1. The two vessels (I and J) are made of pressure-resistant glass (up to 2 MPa); one is a 20-mL vessel for measuring the volume of liquid ammonia (ammonia vessel), and the other is a 100-mL vessel for determining the densities (reaction vessel) that can be agitated by a magnetic stirrer (B).

Two vessels were immersed in a constant-temperature water bath separately, and its accuracy was within ±0.05 °C. The pressure in the reaction vessel was measured by a strain gauge transducer (A) with a accuracy of 0.1% of full scale (2 MPa).

0021-9568/91/1736-0277$02.50/0 © 1991 American Chemical Society

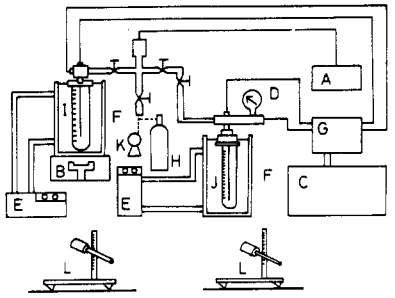

Figure 1. Schematic diagram of the experimental apparatus: (A) digital pressure gauge; (B) magnetic stirrer; (C) recorder; (D) Bourdon gauge; (E) water bath; (F) thermocouple; (G) selective switch; (H) ammonia vessel; (K) vacuum pump; (L) microscope.

The volume of the solution and the liquid ammonia were measured by microscopes (L) within ±0.02% of the full volume. The temperatures in the vesseles and pipe arrangement were measured by chromel–alumel thermocouples (F) corrected by a standard mercury thermometer. The temperature in the vessel was kept within ±0.05 °C.

After a weighed amount of solid material (maximum 0.04 kg) was charged in the reaction vessel, the pipe arrangement and two vessels were kept at 80 °C under vacuum for 2 h in order to remove the moisture from the system. Then, these vessels were cooled to normal temperature. Chilling the ammonia vessel allowed liquid ammonia to be introduced into the ammonia vessel from an ammonia cylinder. Thereafter, the ammonia vessel was kept at 25 °C. Then, the liquid ammonia was transferred to the reaction vessel from the ammonia vessel of different temperature so as to dissolve ammonium halide in the reaction vessel. The density and concentration were determined from the weight of the solvent and solute and also from the volume of solution in the reaction vessel. The quantity of liquid ammonia transferred to the reaction vessel from the ammonia vessel and the volume of solution in the reaction vessel were measured by reading the scales of these two vessels with use of a microscope, respectively. In the case of a saturated solution, most of the ammonium halide dissolved in the liquid ammonia. Then, all valves were closed, and the temperature of reaction vessel was raised slowly at the rate of 0.5 °C/min to dissolve the solute. When the solution of ammonium halide was around saturation, the rate was decreased to 0.2 °C/min or less. The saturated temperature were read at the point where the last crystal disappears. The liquid level in the reaction vessel was also noted immediately. Then, the solution in the reaction vessel was cooled gradually from a temperature higher than the saturated point, and the temperature at which the first crystal appears was recorded. The average of the these two densities was determined as the density of the saturated solution.

In order to prevent the condensation of ammonia gas, a heating coil was rolled around the pipe arrangement and was kept at constant temperature. The correction for the weight of ammonia in the pipe arrangement was calculated by using the equation of state for ammonia gas by Meyer and Jessup (*5*).

Viscosity Measurement. As the NH_4Br–NH_3 and NH_4I–NH_3 systems are high-pressure and corrosive solutions, viscosity measurements of these solutions are not so easy. For this purpose, the falling-body viscometer with use of a He–Ne laser was specially assembled in our laboratory. Figure 2 shows the experimental apparatus of the viscometer. The diameter and height of the cylinder were 1.270×10^{-2} m and 0.45 m, respectively. The two lights of the He–Ne laser (A) were inserted into the cylinder from the two pressure-resistant glass windows (C). The length of the two windows was 2.0×10^{-2} m. Then, the light coming from the cylinder was detected by the photo-

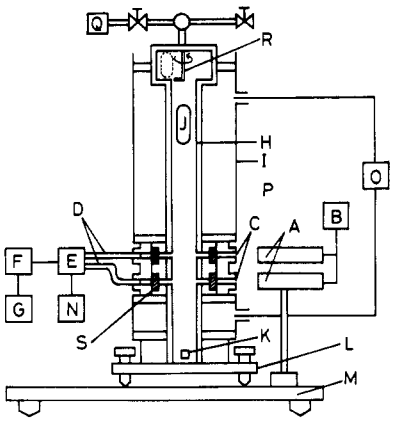

Figure 2. Schematic diagram of the experimental apparatus: (A) He–He laser; (B) water bath; (C) optical window; (D) optical fiber; (E) detector circuit; (F) digital oscilloscope; (G) electric counter; (H) cylinder; (I) water bath; (J) falling body; (K) collector; (L) mount; (M) optical bench; (N) power supply; (O) circulator; (P) Ranthanet magnet.

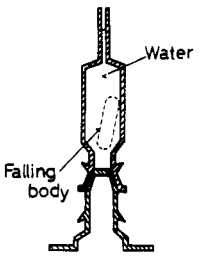

Figure 3. Glass vessel for the volume measurement of a falling body.

transister through the optical fiber (D), the diameter of which was 1.0×10^{-3} m. The signals detected by the phototransister were analyzed using a digital storage oscilloscope and a digital electric counter. If the falling body passed through the glass window, laser light was intercepted by the falling body in the cylinder, and the time required for passing between the two glass windows could be measured. The terminal velocity of the falling body was calculated from the length between the two glass windows and the passing time. The digital resolution of the time measurement was 0.1 μs.

The upper part of the sealed cylinder could be charged with four falling bodies (each body with different density) at the same time. After the experiment, the falling body at the bottom of cylinder was pulled up by using a Ranthanet magnet collector sealed with Teflon. Furthermore, the cylinder was covered with a constant-temperature water bath, with an accuracy within ±0.05 °C.

Figure 3 shows the glass vessel for the measurement of the volume of the falling body. At first, this glass vessel was filled with water at 25 °C up to a fixed line. Thereafter, the falling body was placed in the apparatus, and the glass vessel was again filled with water up to the fixed line. The volume of the falling body was calculated from the difference of its weight and the mass difference of this vessel.

For the experiment, after a weighed amount of solid material was charged in the stainless steel cylinder, it was kept at 80 °C under volume for 2 h in order to remove the moisture from the system. Then, these vessels were cooled to normal temperature. Chilling the ammonia vessel (its volume was 10^{-3} m^3) allowed liquid ammonia to be introduced into the ammonia vessel from the ammonia cylinder. Thereafter, the ammonia vessel and cylinder were kept at 40 and 0 °C, respectively, and liquid ammonia was transferred to the cylinder from the ammonia vessel. The quantity transferred to the cylinder from the ammonia vessel was determined from weight difference of the ammonia vessel. Its accuracy were within 0.001 g. The mass

Table I. Densities (ρ) of the NH_4Br–NH_3 System at Various Temperatures

mass % of NH_4Br	ρ, kg/m³					
	0 °C	10 °C	20 °C	30 °C	40 °C	50 °C
9.8	706	695	681	669	653	637
19.7	780	769	755	743	726	714
30.1	865	854	843	829	816	807
40.5	948	941	927	916	903	891
50.2	1051	1043	1033	1023	1014	997
60.8	1168	1159	1147	1137	1125	1114

Table II. Densities (ρ) of the NH_4I–NH_3 System at Various Temperatures

mass % of NH_4I–NH_3	ρ, kg/m³					
	0 °C	10 °C	20 °C	30 °C	40 °C	50 °C
10.1	710	700	694	681	666	649
19.8	794	785	776	764	750	737
30.4	890	881	871	862	851	837
40.2	993	986	977	968	957	943
49.9	1109	1101	1094	1084	1073	1061
60.3	1239	1230	1223	1211	1203	1192
69.8	1373	1349	1326	1302	1280	1257

Table III. Coefficients a_i, b_j for Least-Squares Representations of Density

	NH_4Br–NH_3 system			NH_4I–NH_3 system		
	a_0	a_1	a_2	a_0	a_1	a_2
b_0	0.638412	-1.38182×10^{-3}	-2.6147×10^{-6}	0.638905	-1.35588×10^{-3}	-3.45319×10^{-6}
b_1	6.92786×10^{-3}	7.77802×10^{-5}	-1.20299×10^{-6}	6.50616×10^{-3}	1.46554×10^{-4}	-1.25946×10^{-3}
b_2	7.18433×10^{-6}	-6.39803×10^{-6}	1.13774×10^{-7}	5.72231×10^{-5}	-9.30585×10^{-6}	7.50838×10^{-8}
b_3	3.64899×10^{-7}	1.78457×10^{-7}	-3.17576×10^{-9}	2.97606×10^{-9}	2.19404×10^{-7}	1.55015×10^{-9}
b_4		-1.52249×10^{-9}	2.68685×10^{-11}		-1.70813×10^{-9}	1.07121×10^{-11}

percent of the solution was determined from each weight.

The falling-body viscometer is a popular and simple viscometry apparatus. By utilizing Stokes equation for a falling body under the influence of gravity in an infinite Newtonian fluid medium, the time difference (Δt) for passing through the two points in the cylinder, the densities of the falling body and fluid (ρ_s, ρ_f), and the geometry constant (K) were needed to calculate the viscosity from the following relation:

$$\mu = K(\rho_s - \rho_f)\Delta t \quad (1)$$

The geometry constant K was expressed as a function of the form of the falling body and diameter of cylinder. K was determined from some standard liquids for calibrating viscometers. The reproducibility of geometry constant measurements was within ±1.5%. The viscosities were calculated from eq 1. For confirmation of whether or not the observed velocity was the terminal velocity, two falling bodies were tested in the same fluid. If the density (ρ_f) of the solution, obtained from eq 2, was

$$K_1(\rho_{s1} - \rho_f)\Delta t_1 = K_2(\rho_{s2} - \rho_f)\Delta t_2 \quad (2)$$

in agreement with the density determined from its initial weight and mass within a accuracy of ±0.5%, the observed viscosity was adopted for use in this experiment.

Result and discussion

Density. The densities of the NH_4Br–NH_3 and NH_4I–NH_3 systems are shown in Tables I and II. All density data were fitted to a quadratic correction, given as eq 3 and 4.

$$\rho = 1000\left(\sum_{j=0}^{2} a_j T^j\right) \quad (3)$$

$$a_j = \sum_{j=0}^{4} b_j X^j \quad (4)$$

Values for a_j and b_j are listed in Table III. Smoothed values calculated from this equation agreed with the observed data within ±0.5%. Table IV shows the densities of the saturated solution for the NH_4Br–NH_3 and NH_4I–NH_3 systems. The accuracy of the density measurement was estimated within ±0.1%, judging from the accuracy of microscope.

Table IV. Densities of Saturated Solutions for the NH_4Br–NH_3 and NH_4I–NH_3 Systems

NH_4Br–NH_3 system			NH_4I–NH_3 system		
temp, °C	concn,[a] %	density, kg/m³	temp, °C	concn,[a] %	density, kg/m³
0	68.58	1268	0	77.05	1526
1.7	68.70	1269	6.1	77.39	1531
6.0	69.01	1271	10.0	77.63	1534
11.6	69.42	1274	15.5	77.97	1540
16.3	69.89	1277	19.9	78.26	1545
20.1	70.25	1279	24.8	78.60	1551
26.0	70.87	1282	30.2	79.01	1558
29.9	71.31	1284	34.9	79.38	1564
33.0	71.68	1286	38.7	79.71	1570
34.5	71.86	1287	40.9	79.90	1573
35.2	71.92	1288	43.5	80.14	1576
40.9	72.08	1289	45.2	80.30	1579
44.6	72.18	1290	50.4	80.82	1587
51.7	72.39	1292	55.5	81.37	1595
58.5	72.60	1295	59.0	82.38	1601
63.7	72.76	1296	63.9	82.38	1609
69.6	72.95	1298	68.2	82.95	1616
76.5	73.18	1302	69.4	83.11	1618

[a] Mass percent of solute (NH_4Br or NH_4I).

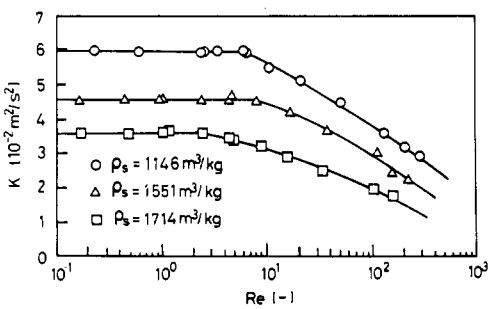

Figure 4. Relation between geometry constant K and Re.

Viscosity. Figure 4 shows the relation between the geometry constant (K) and the Reynolds number. These constants

Table V. Viscosities (μ) of the NH_4Br–NH_3 System at Various Temperatures

mass % of NH_4Br	μ, Pa s				
	10.0 °C	20.0 °C	30.0 °C	40.0 °C	50.0 °C
10.0	0.208	0.191	0.177	0.156	0.140
21.7	0.316	0.280	0.252	0.224	0.210
30.2	0.485	0.398	0.351	0.308	0.280
40.9	0.781	0.682	0.595	0.517	0.452
49.5	1.390	1.163	1.011	0.877	0.755
59.8	3.535	2.843	2.310	1.810	1.461

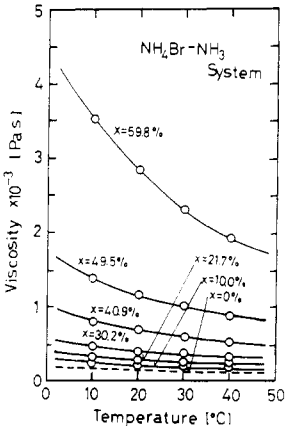

Figure 5. Viscosities of the NH_4Br–NH_3 system.

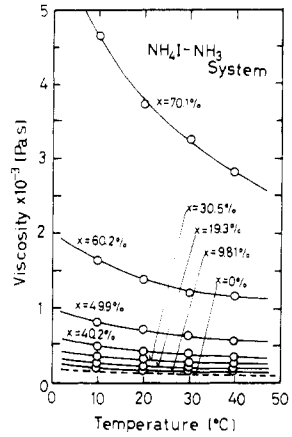

Figure 6. Viscosities of the NH_4I–NH_3 system.

(K) were determined from eq 1, as shown in Figure 4. These data were constants under $Re = 3$, and the experiment was carried out in the range of $Re < 2$.

The observed viscosities are listed in Tables V and VI, and Figures 5 and 6 show the temperature dependence on the viscosity of NH_4Br–NH_3 and NH_4I–NH_3 systems. The plots of logarithms of the viscosity against the reciprocal of the absolute temperature for solutions give straight lines being nearly parallel. The accuracy of this falling-body viscometer was within ±1.2%, judging from the measurements of standard reference materials.

Table VI. Viscosities (μ) of the NH_4I–NH_3 System at Various Temperatures

mass % of NH_4I	μ, Pa s				
	10.0 °C	20.0 °C	30.0 °C	40.0 °C	50.0 °C
9.81	0.195	0.178	0.162	0.146	0.138
19.3	0.244	0.222	0.201	0.182	0.170
30.5	0.345	0.312	0.282	0.250	0.230
40.2	0.490	0.438	0.395	0.348	0.315
49.9	0.811	0.710	0.634	0.557	0.498
60.0	1.360	1.382	1.220	1.118	0.972
70.1	4.625	3.720	3.243	2.800	2.430

Conclusion

The density and viscosity of NH_4Br–NH_3 and NH_4I–NH_3 were measured over a wide range of temperatures and concentrations. The experimental apparatuses used in this paper were special equipment assembled to facilitate measurements at high pressure.

Nomenclature

a = coefficient of least-squares equation
b = coefficient of least-squares equation
K = geometry constant defined in eq 1 (cm^2/s^2)
t = time difference (s)
T = temperature (°C)
X = mass percent of solute (%)

Greek Letters

μ = viscosity (Pa s)
ρ = density (kg/m^3)

Subscripts

f = fluid
s = solid
1 = number of falling body
2 = number of falling body

Registry No. NH_3, 7664-41-7; NH_4Br, 12124-97-9; NH_4I, 12027-06-4.

Literature Cited

(1) Macliden, M. O.; Klein, S. A. *Solar Energy* **1983**, *31* (5), 473–482.
(2) Yamamoto, H.; Sanga, S.; Tokunaga, J. *Ind. Eng. Chem. Res.* **1987**, *26*, 2389–2393.
(3) Yamamoto, H.; Tokunaga, J.; Sanga, S. *J. Chem. Eng. Data* **1986**, *31*, 283–285.
(4) Yamamoto, H.; Sanga, S.; Tokunaga, J. *J. Chem. Eng. Data* **1988**, *33*, 381–385.
(5) Meyer, C. H.; Jessup, R. S. *Refrig. Eng.* **1924**, *11*, 348.

Received for review May 23, 1990. Revised October 2, 1990. Accepted November 26, 1990.